ACS OMEGA

http://pubs.acs.org/journal/acsodf

Article

Integrative Proteomic and Phosphoproteomic Analyses Revealed the Regulatory Mechanism of the Response to Ultraviolet B Stress in *Clematis terniflora DC*

Minglei Tao, Shengzhi Liu, Amin Liu, Yaohan Li, Jingkui Tian, Bingxian Yang,* and Wei Zhu*

Cite This: *ACS Omega* 2023, 8, 1652−1662

Read Online

ACCESS | Metrics & More | Article Recommendations | Supporting Information

ABSTRACT: *Clematis terniflora DC.* (*C. terniflora*) has been used as an ancient Chinese traditional herbal medicine. The active substances in *C. terniflora* have been confirmed to be effective in treating diseases such as prostatitis. UV light radiation is a common environmental factor that damages plants and influences primary and secondary metabolism. Previous studies showed that ultraviolet B (UV-B) radiation followed by dark stress resulted in the accumulation of secondary metabolites in *C. terniflora* leaves. An in-depth understanding of how *C. terniflora* leaves respond to UV-B stress is crucial for improving *C. terniflora* value. Here, we conducted label-free proteomic and phosphoproteomic analyses to explore the protein changes under UV-B and UV-B combined with dark treatment. A total of 2839 proteins and 1638 phosphorylated proteins were identified. Integrative omics revealed that the photosynthetic system and carbohydrate balance were modulated under both stresses. The phosphoproteomic data indicated that the mitogen-activated protein kinase signaling pathway was triggered, while the abundance of phosphorylated proteins related to osmotic stress was increased under UV-B stress. Differentially abundant phosphoproteins from UV-B followed by dark treatment were mainly enriched in response to stimulus including calcium-mediated proteins. This study provides new insight into the impact of UV-B stress on *C. terniflora* and plant molecular resistance mechanisms through proteomic and phosphoproteomic analyses.

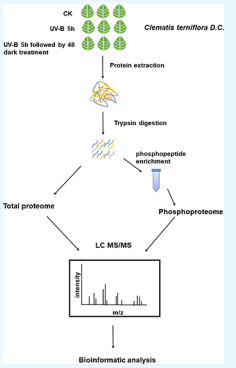

1. INTRODUCTION

Clematis terniflora DC. (*C. terniflora*) is a kind of woody vine of *Clematis* L. that is mainly distributed in China, Japan, and Europe. It is widely used as an ornamental plant and has high application value in horticulture. In addition, *C. terniflora* has been famous as folk medicine for a long time in China, and its stems, leaves, and roots contain a variety of active ingredients such as coumarins, flavonoids, and alkaloids.[1−3] It has been used to treat rheumatoid arthritis, chronic pharyngitis, and inflammatory symptoms in the respiratory and urinary systems. Flavonoids extracted from the aerial part of *C. terniflora* are reported to be effective in treating prostatitis.[4] The results of pharmacological experiments showed that tumor growth can be inhibited by the active ingredient isolated from *C. terniflora*.[5]

For decades, researchers have been devoted to discovering the influential mechanism of ultraviolet B (UV-B) on plants. UV-B radiation usually causes damage to DNA, proteins, and plant morphological features. One of its major negative influences is triggering the accumulation of reactive oxygen species (ROS) in cells. UV-B radiation increased the abundance of antioxidases, such as superoxide dismutase in soybeans.[6] In *Catharanthus roseus*, the calcium-related pathway and ROS scavenging system were activated under UV-B stress.[7] Moreover, UV-B stress also has the potential to increase the secondary metabolite contents, which can be used by plants for stress resistance.[8] Berberine, jateorhizine, palmatine, and columbamine were increased when *Mahonia bealei* was exposed to UV-B radiation combined with dark treatment.[9] It has been reported that the concentration of kaempferol increases after UV-B radiation in *Arabidopsis thaliana*.[10] UV-B followed by dark treatment also increased the contents of coumarins in *C. terniflora* according to a previous study,[11] and the ATP content increased to provide energy for secondary metabolism.[3] Therefore, exposure to UV-B stress might contribute to the increase in active ingredients, thereby elevating the quality of folk medicine.[12] However, the induction and response mechanism of *C. terniflora* is not fully understood.

Protein phosphorylation is catalyzed by protein kinases, which transfer the phosphate group of ATP/GTP to the protein amino acid residue.[13] This posttranslational modification (PTM) is one of the most well-studied protein modifications. Protein phosphorylation is involved in many signal recognition and transduction pathways in plants. In *Arabidopsis thaliana*, the phosphorylation of tyrosine regulates the oxidative stress pathway in response to drought and salt stress.[14] The mitogen-activated protein kinase (MAPK) signaling pathway transfers signals to downstream molecules through phosphorylation, and it can be activated by ROS, calcium (Ca^{2+}), and

Received: November 11, 2022
Accepted: December 21, 2022
Published: December 29, 2022

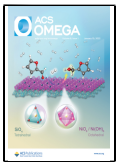

phytohormones. Proteomics combined with phosphoproteomics has become a major way to investigate plant resistance mechanisms under biotic and abiotic stress. For example, multiomics studies have explored the *Spongospora subterranea* resistance mechanisms of potato and identified that protein phosphorylation plays a role in the regulation of the immune response.[15] Integrative proteomic and phosphoproteomic analyses showed that the early cold response in maize was associated with photosynthetic light reactions and the spliceosome.[16] Nevertheless, no research has combined proteomic and phosphoproteomic to study the molecular mechanism controlling changes in *C. terniflora* under UV-B stress.

Phosphorylation may help *C. terniflora* respond to abiotic stress through a regulation mechanism. In this study, we integrated proteomic and phosphoproteomic analyses to further expand the understanding of *C. terniflora* leaves in response to UV-B treatment. The data of this study revealed the differentially abundant proteins and phosphoproteins between UV-B treated and untreated plants, which will help to infer the phosphorylation regulation mechanism. The results of this study provide new insights into the signal transduction of *C. terniflora* abiotic responses.

2. MATERIALS AND METHODS

2.1. Plant Growth and Treatment. *C. terniflora* plants were obtained from a greenhouse and grown at 25 °C under white light. Leaves of different groups, control (CK), 5 h ultraviolet B treatment (UVB), and 5 h ultraviolet B followed by 48 h dark treatment (UVD), were collected as reported previously.[3] For proteomics analysis, three independent biological replicates were performed per treatment.

2.2. Analysis of Total Soluble Sugar Contents, Total Antioxidant Capacity (T-AOC), and Chlorophyll Contents. The total soluble sugar contents of CK, UVB, and UVD were measured with a plant soluble sugar content test kit (Solarbio, Beijing, China) according to the instructions. The absorbance of each sample was measured at 620 nm, and the content of soluble sugar was calculated on the basis of a standard curve. The T-AOC and chlorophyll content of each group were determined colorimetrically by a total antioxidant capacity assay kit (Nanjing Jiancheng Bioengineering Institute, Nanjing, China) and chlorophyll assay kit (Nanjing Jiancheng Bioengineering Institute). Chlorophyll content determination was performed with 0.1 g leaf samples. The absorbance values at OD_{645} and OD_{663} were measured. The calculation formula are as follows: (1) chlorophyll a = $(12.7 \times OD_{663} - 2.69 \times OD_{645}) \times$ volume × dilution rate/(sample weight × 1000). (2) Chlorophyll b = $(22.9 \times A645 - 4.68 \times A663) \times$ volume×dilution rate/(sample weight × 1000). (3) Total chlorophyll content = chlorophyll a content + chlorophyll b content. T-AOC content measurement was performed after incubating the sample and mix buffer at 37 °C for 30 min. At least three independent biological replicates were performed per treatment.

2.3. Protein Sample Preparation and Phosphopeptide Enrichment. Frozen leaves ground into powder were transferred to extraction solution (100 mM KCl, phosphatase inhibitor cocktails (Roche Diagnostics, NSW, Australia), 5 mM EDTA, 1% (w/v) DTT, 1 mM PMSF, 30% sucrose, and 50 mM Tris−HCl at pH 8.5). Tris-buffer phenol was added to the mixture, and the mixture was centrifuged at 6000 × *g*. Five volumes of 100 mM ammonium acetate were added to the protein supernatant and precipitated at −20 °C over 12 h. After centrifugation at 6000 × *g* for 10 min, the precipitate was collected and then washed twice with acetone. The precipitate was dissolved in buffer containing 7 M urea, 2 M thiourea, 4% CHAPS, 2 mM EDTA, 10 mM DTT, and 1 mM PMSF. The supernatant was collected after centrifugation as crude protein. The Bradford method was used for protein concentration determination with minor modifications. Protein purification, reduction, and alkylation were performed according to previous study.[17] In brief, protein was purified by methanol and chloroform and then dissolved in NH_4HCO_3. Finally, trypsin was added at a 1:50 (trypsin-to-protein) ratio, and the sample was incubated at 37 °C for 16 h in the dark to digest protein and then desalted with a Strata X column (Phenomenex, United States) to obtain total peptide samples and phosphopeptide enrichment prior samples. The TiO_2 phosphopeptide enrichment kit (PTM BioLab, Hangzhou, China) was used to enrich the peptide according to the manufacturer's instructions.

2.4. LC−MS/MS Analysis. Peptides were redissolved in solvent A (0.1% formic acid) and analyzed by an Orbitrap Exploris 480 mass spectrometer (Thermo Fisher Scientific Inc., San Jose, CA, USA), using an Acclaim PepMap 100 C18 column (25 cm × 75 μm, 2 μm-C18, Thermo Fisher Scientific Inc.). The peptides were separated by a Thermo Easy-nLC 1000 system. The parameters and gradient setting were in accordance to Zhong et al.'s[18] protocol with minor modification. The gradient started at 3% solvent B (acetonitrile), 3% B to 8% B for 1 min, 8% B to 45% B for 101 min, and 45% B to 95% B for 4 min and finally held at 95% for 9 min. The flow rate was 300 nL/min, and the column temperature was 40 °C.

2.5. Data Processing and Bioinformatics Analysis. Raw data files were searched using the SEQUEST HT search engine embedded into Proteome Discoverer version 2.4 (Thermo Scientific). Spectral libraries were generated by searching the Uniprot database (Raninculales, 233,260 entries, 2022.6.15) and *C. terniflora* DC. transcriptome database.[19] Trypsin/P was configured as a cleavage enzyme (up to 2 missing cleavages), and the false discovery rate (FDR) was set at a 1% cutoff. For the phosphoproteomic search, phosphoRS mode was enabled, phospho (S/T/Y) was specified as an additional variable modification, and default settings were used for other modifications. Relative quantitation of total proteins or phosphoproteins was performed according to the respective peptides or phosphopeptides.

The proteins with an adjusted p value of <0.05 and a fold change of >1.2 or <0.83 were considered as differentially abundant proteins (DAPs) with statistical significance. Differentially phosphorylated proteins (DPPs) were identified using the same screening method, and overlapping proteins with the same change trend between DAPs and DPPs were deleted. Functional annotations of DAPs or DPPs were performed by an eggNOG-mapper,[20] based on Gene Ontology (GO). GO term enrichment was performed by TBtools software.[21] DAPs and DPPs were submitted to the online KOBAS 3.0[22] software for Kyoto Encyclopedia of Genes and Genomes (KEGG) pathway enrichment. Subcellular prediction was performed by WoLF PSORT (https://wolfpsort.hgc.jp/).

2.6. Statistical Analysis. Statistical differences between three groups were tested using one-way ANOVA together with Tukey's test in SPSS (version 25). Student's t test was used to evaluate statistical significance between two groups. Data are expressed as the means ± SDs.

https://doi.org/10.1021/acsomega.2c07258
ACS Omega 2023, 8, 1652−1662

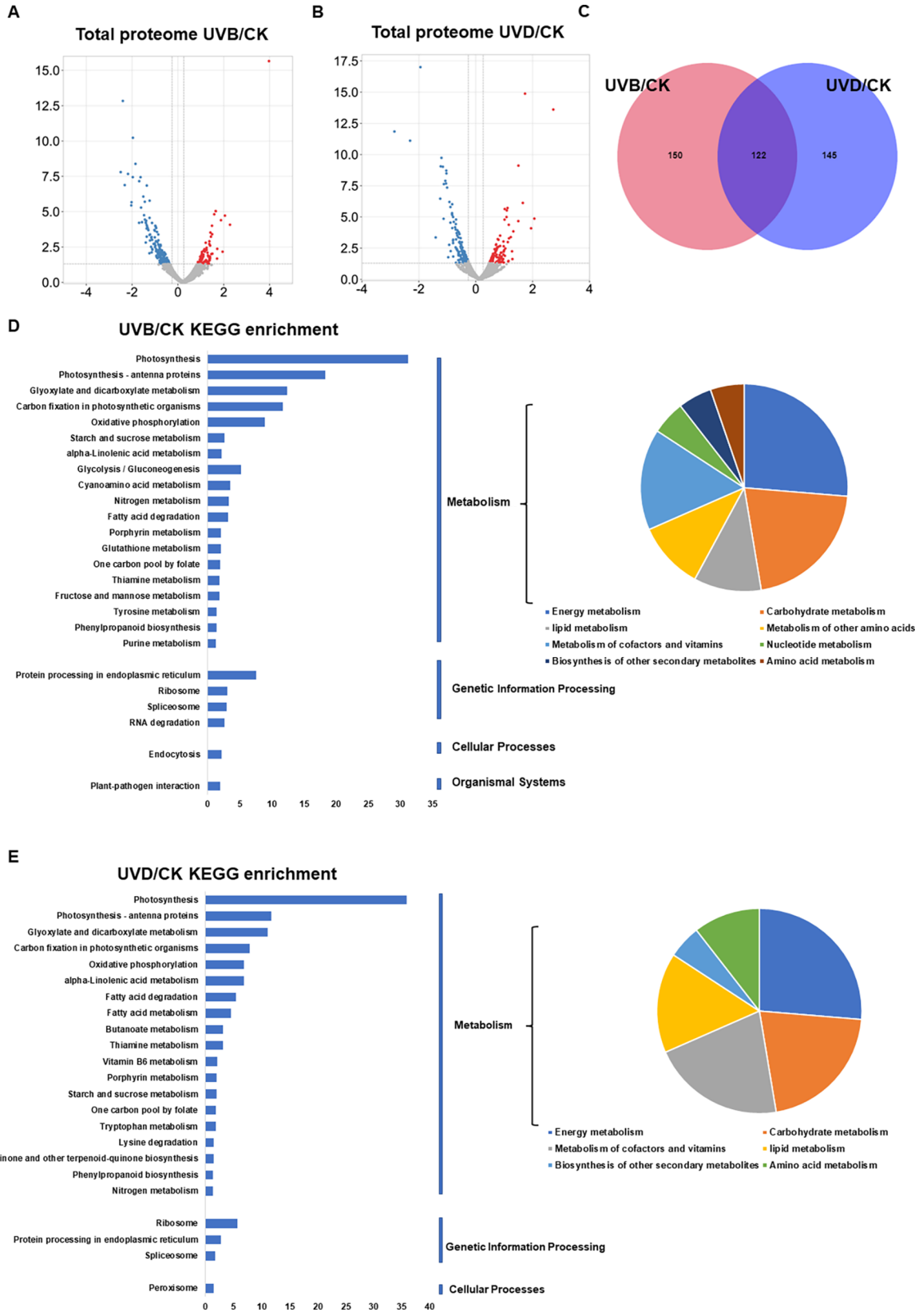

Figure 1. Differentially abundant proteins (DAPs) identified in response to UVB and UVD stresses. Volcano maps of DAPs in (A) UVB/CK and (B) UVD/CK. Red dots refer to increased DAPs, and blue dots refer to decreased DAPs. (C) Venn diagram shows the overlap of DAPs under two different treatments. Bar chart of significantly enriched KEGG pathways of DAPs in (D) UVB/CK and (E) UVD/CK. The *x* axis of (D) and (E) represents −log10 (*p* value) of KEGG enrichment significance.

https://doi.org/10.1021/acsomega.2c07258
ACS Omega 2023, 8, 1652−1662

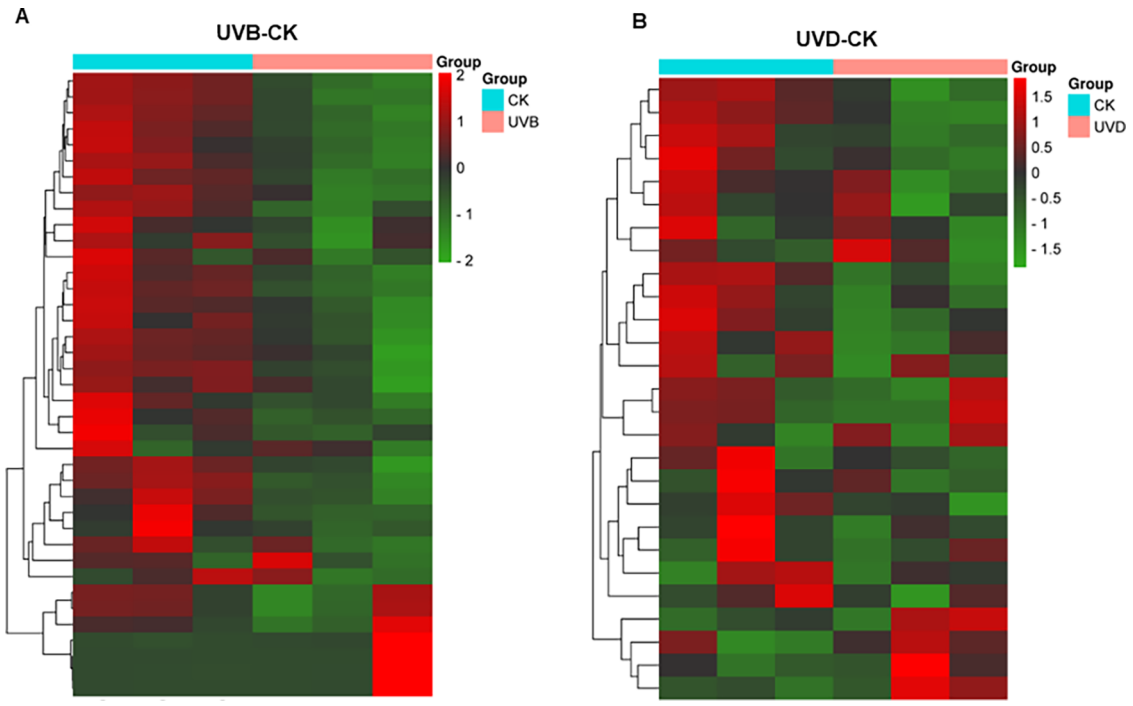

Figure 2. Clustering heatmap of DAPs related to photosynthesis and photosynthesis−antenna protein pathways. (A) DAPs in UVB/CK. (B) DAPs in UVD/CK.

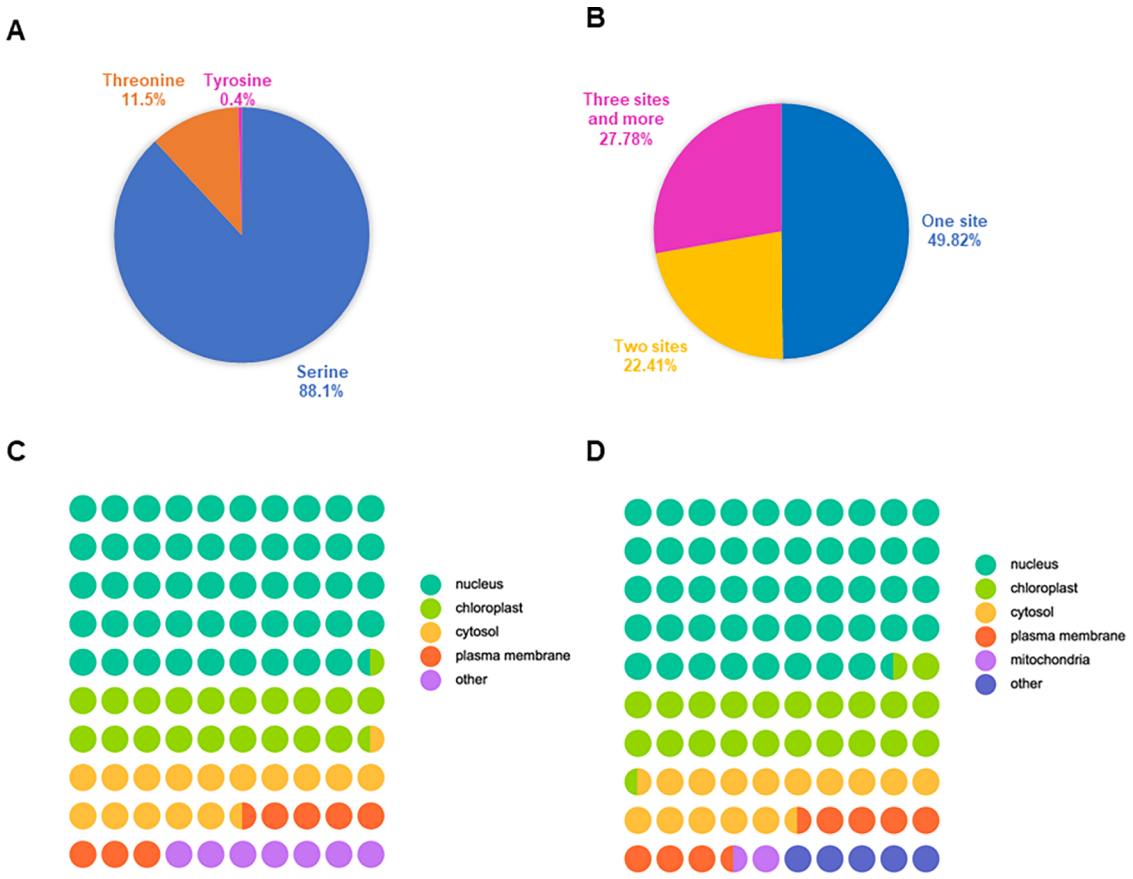

Figure 3. Statistical information of phosphorylation sites and subcellular localization of differentially phosphorylated proteins. Distribution of (A) phosphorylated sites (serine, Ser; threonine, Thr; tyrosine, Tyr) in identified phosphoproteins. (B) Proportion of phosphorylation site numbers per identified phosphoprotein. The subcellular localization of DPPs of (C) UVB/CK and (D) UVD/CK predicted by WoLF PSORT.

https://doi.org/10.1021/acsomega.2c07258
ACS Omega 2023, 8, 1652−1662

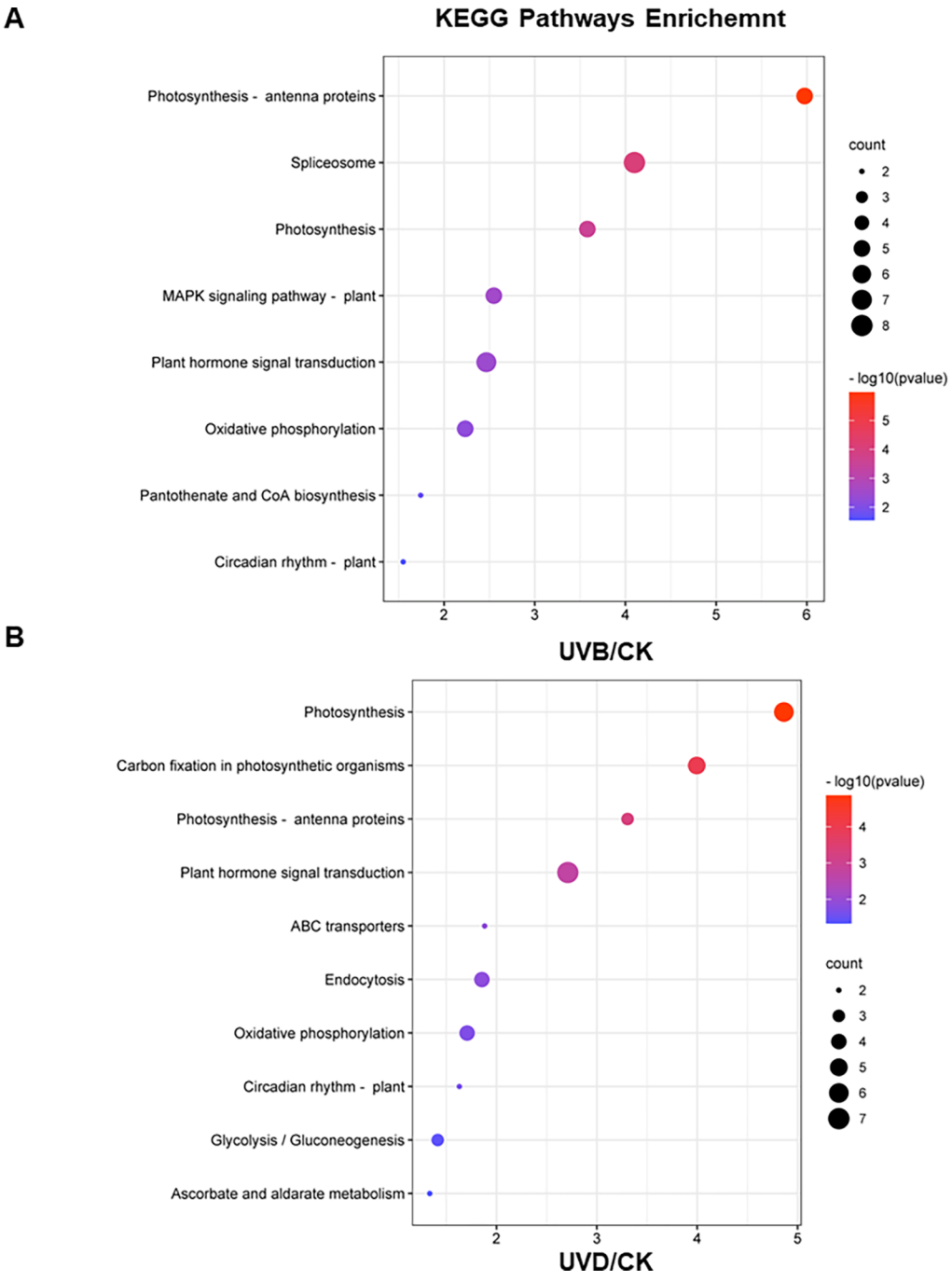

Figure 4. Bubble plot of significantly enriched KEGG pathways of DPPs in (A) UVB/CK and (B) UVD/CK. The color of the bubble represents the −log10 (p value) of KEGG enrichment significance. The size of the bubble represents the number of DPPs.

3. RESULTS

To explore the roles of proteins and phosphorylated proteins in *C. terniflora* under UV-B stress, we collected UVB-treated and UVD-treated leaf proteins, and the proteomic and phosphoproteomic were profiles by using an LC−MS/MS approach.

3.1. Overview of *C. terniflora* Proteomics under UV Stress. In the global proteome, a total of 2839 proteins were identified in the CK, UVB, and UVD groups. In comparison with leaves from the CK group, based on a p value of <0.05 and a fold change ratio of >1.2 or <0.83, leaves in UVB/CK had 272 DAPs (increased/decreased: 86/186), and leaves in UVD/CK presented 267 DAPs (increased/decreased: 116/151) (Figure 1A,B). Noticeably, 122 DAPs were identified under both UVB and UVD stresses, while over half of the DAPs changed specifically under the two different stresses (Figure 1C).

GO classification of the DAPs according to molecular function (MF) and biological process (BP) ontological terms was performed. The top 20 GO enrichment terms in each category are shown in Figure S1A,B. Tissue development and cellular metabolic compound salvage were the top two BP categories in which UVB DAPs were enriched. DAPs in UVD were associated with the transport of organophosphate esters and organic anions and lipid oxidation-related categories. Both groups of DAPs were enriched in the response to the light/abiotic stimulus. In MF, UVB DAPs were more related to DNA binding and sequence-specific DNA binding, while transporter

https://doi.org/10.1021/acsomega.2c07258
ACS Omega 2023, 8, 1652−1662

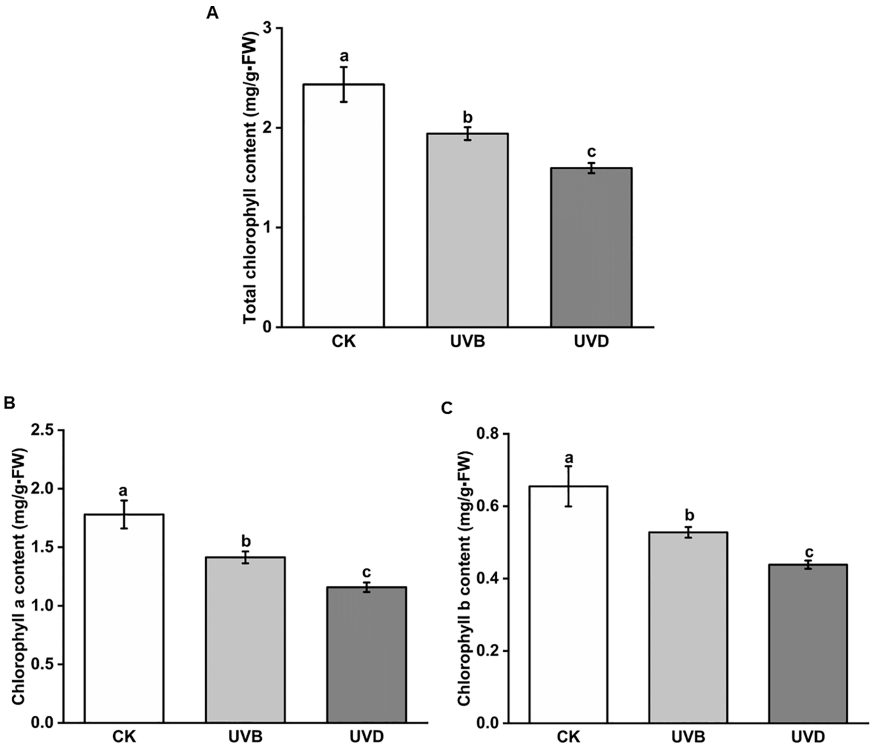

Figure 5. Levels of (A) total chlorophyll, (B) chlorophyll a, and (C) chlorophyll b of *C. terniflora* leaves from CK, UVB, and UVD groups. The different letters indicate significant differences according to one-way ANOVA.

activity and protein binding were the most common terms in UVD DAP enrichment.

Based on the KEGG pathway enrichment analysis of UVB DAPs, the most significantly enriched pathways were photosynthesis and photosynthesis−antenna proteins. Other enriched pathways were carbohydrate metabolism pathways such as glyoxylate and dicarboxylate metabolism, starch and sucrose metabolism, and glycolysis/gluconeogenesis (Figure 1D). Except for energy metabolism pathways and carbohydrate metabolism pathways, some lipid metabolism pathways (such as alpha-linolenic acid metabolism, fatty acid degradation, and fatty acid metabolism) also ranked highly among the enriched pathways in UVD (Figure 1E). Furthermore, we found that DAPs were enriched in the phenylpropanoid biosynthesis pathway in both UVB and UVD, which meant that secondary metabolism was affected. Overall, the enriched pathways were mainly associated with metabolism, especially energy metabolism and carbohydrate metabolism.

Photosynthesis and photosynthesis−antenna proteins were the top two enriched pathways in UVB/CK and UVD/CK. Therefore, we selected DAPs mapped to these two pathways in response to UVB and UVD. Figure 2 illustrated that, compared to the control group, the abundance of most proteins in the photosynthesis system were decreased under stress.

3.2. Phosphoproteomic Analysis of *C. terniflora* Leaves in Response to UV Stress. In the phosphoproteomic analysis, we detected 1638 phosphorylated proteins, of which 238 (134 increased and 104 decreased) proteins in UVB and 218 (83 increased and 135 decreased) proteins in UVD significantly changed in abundance compared to those in the control group. Among the 1638 phosphoproteins, 3752 phosphorylation sites were identified. The distribution of phosphorylation sites was 88.1% Ser, 11.5% Thr, and 0.4% Tyr (Figure 3A). In this study, 49.8% of phosphoproteins were due to single phosphorylation, 22.4% were due to double phosphorylation, and the rest had three or more phosphorylation sites (Figure 3B).

Subcellular localization prediction analysis showed that nearly 50% of the significantly changed phosphoproteins were located in the nucleus, followed by the chloroplast, cytosol, and plasma membrane. The distributions of the subcellular localization of phosphoproteins in UVB (Figure 3C) and UVD (Figure 3D) were similar. The results showed that most of DPPs were nuclear-related proteins, which indicated that phosphorylation of nuclear proteins played an essential role in the response to UV light stress.

GO enrichment revealed that the major effects of UV-B at the phosphoproteomic level involved the hyperosmotic response, plant organ development, and response to oxygen-containing compound in the BP category; plant-type vacuole in the CC category; and active transmembrane transporter activity in the MF category (Figure S2A). In contrast, the majority of significantly changed phosphoproteins of UVD were related to the response to stimulus/water deprivation and DNA-binding transcription factor activity (Figure S2B).

KEGG enrichment pathways of DPPs in UVB were not only associated with photosynthesis-related energy metabolism pathways but also related to transcription and signal transduction. Specifically, these KEGG pathways were spliceosome, MAPK signaling pathway−plant, and plant hormone signal transduction (Figure 4A). The KEGG pathway enrichment results revealed that ten pathways were significantly enriched, including photosynthesis, carbon fixation in photosynthetic organisms, photosynthesis−antenna proteins, plant hormone signal transduction, ABC transporters, and so on (Figure 4B).

3.3. Effects of UV-B Radiation on Chlorophyll, Soluble Sugar, and T-AOC Levels. To investigate the photosynthetic response to the UV-B stress on *C. terniflora* leaves, we measured the chlorophyll content (Figure 5A). The results showed that

https://doi.org/10.1021/acsomega.2c07258
ACS Omega 2023, 8, 1652−1662

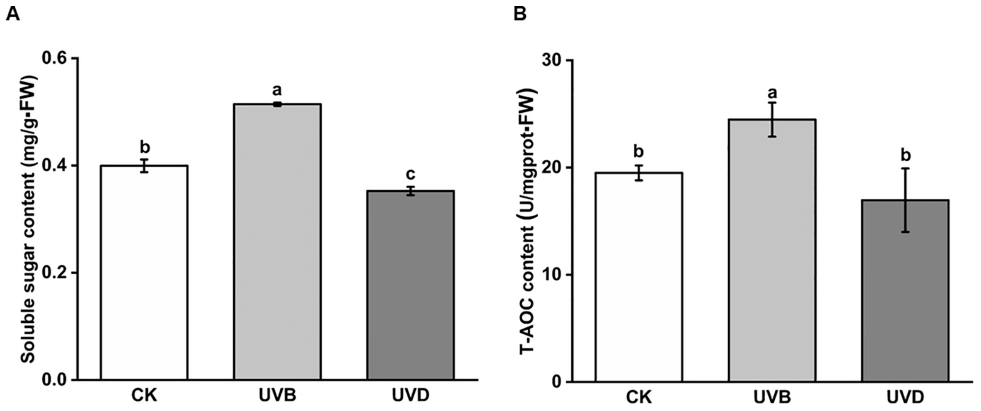

Figure 6. (A) Soluble sugar content and (B) T-AOC content change in different groups of *C. terniflora* (CK, UVB, and UVD). Letters a, b, and c indicated that the content changed significantly according to one-way ANOVA.

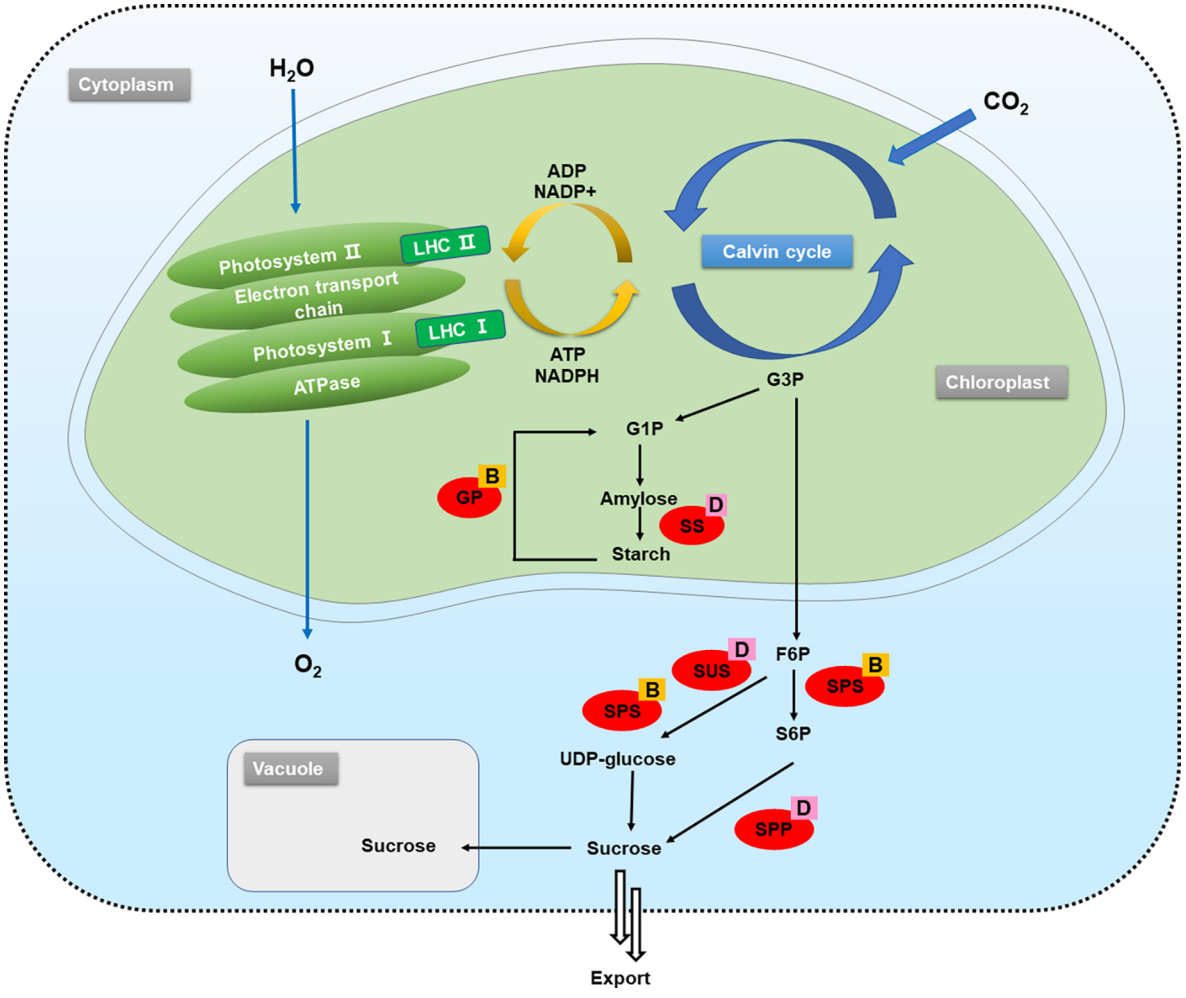

Figure 7. Identified DAPs from UVD/CK and UVB/CK mapped to carbohydrate metabolism. The red ellipses represent increased DAPs. The blocks with the letter "B" inside indicate that the DAP comes from UVB/CK, and those with the letter "D" mean that the DAP comes from UVD/CK. G3P, glyceraldehyde 3 phosphate; G1P, glucose 1 phosphate; F6P, fructose 6-phosphate; S6P, sucrose 6 phosphate; GP, glycogen phosphorylase; SS, starch synthase; SUS, sucrose synthase; SPS, sucrose phosphate synthase; and SPP, sucrose phosphatase.

UV-B radiation reduced the total chlorophyll content in *C. terniflora* leaves. Furthermore, the total chlorophyll content was lower in the UVD group than in the UVB group. Consistent with the change in total chlorophyll, chlorophyll a and chlorophyll b (Figure 5B,C) were decreased in the UVB group and UVD group, respectively.

The plant soluble sugar content and T-AOC were determined using test kits. Figure 6A showed that the content of soluble sugar rose significantly after UVB stress. However, the soluble sugar content declined in the UVD group. For the T-AOC content, the UVB group showed a significantly higher value than the other two groups (Figure 6B).

https://doi.org/10.1021/acsomega.2c07258
ACS Omega 2023, 8, 1652−1662

4. DISCUSSION

In this study, we used proteomic and phosphoproteomic analyses to investigate the response mechanisms of *C. terniflora* response to UV-B light stress. Leaves were treated with UV-B and UV-D separately. Taken together, we identified DAPs and DPPs between the treated and control groups, highlighting the significance of the *C. terniflora* defense regulation system. The results showed how UV-B affected the signal transduction and metabolism systems.

4.1. Photosynthetic Response Was Inhibited in Response to UV-B Stress. Figures 1D,E and 4 reveal that photosynthesis and photosynthesis−antenna proteins were the top two ranked pathways in almost all KEGG enrichment results for the proteomic and phosphoproteomic analyses. Regarding the DAPs and DPPs related to the above two pathways, most proteins in the UVB group and UVD group were downregulated (Figure 2, Tables S1−S4). The antenna protein is also called light-harvesting chlorophyll (LHC) a and b binding protein and has the ability to absorb light energy.[23] Zhang et al. reported that high NH_4^+ stress decreased the expression of *LHC* genes and resulted in a decrease in chlorophyll concentration in *Myriophyllum aquaticum*.[24] Consistent with previous research, we noticed a decline in the chlorophyll content after UV-B stress, and the content was even lower in the UVD-treated samples (Figure 5A). Ferredoxin is involved in chlorophyll metabolism[25] and is an important protein that participates in electron transport in photosynthesis together with ferredoxin NADP reductase (FNR). FNR accepts electrons from ferredoxin and generates NADPH at the end of the photosynthetic electron transfer chain.[26] Owing to the decrease in chlorophyll accumulation, rice mutants of the ferredoxin gene *FdC2* were pale green[27] according to previous research. In a barley mutant with C-type ferredoxin gene disruption, the plant presented a chlorophyll deficient phenotype.[28] High light stress in *Arabidopsis thaliana* showed that FNR abundance was related to PSI inactivation.[29] The overexpression of FNR increased the tolerance to high light and oxidative stress. According to total proteomics data, the abundance levels of ferredoxin and ferredoxin NADP reductase (FNR) were decreased in response to the stresses[30] (Tables S1 and S2). In line with the above analysis, the photosynthesis system may undergo massive damage under UV-B stress in *C. terniflora*.

4.2. Carbohydrate Balance Was Modulated in Resistance UV-B Stress. Carbohydrates are the direct product of photosynthesis, which provides plants with energy.[31] Soluble sugars are required for growth, as well as maintenance of the osmotic homeostasis of cells.[32] However, excess soluble sugars decrease the level of the photosynthesis in *Arabidopsis*.[33] According to the data on total protein levels, the abundance of sucrose synthase (SUS) and sucrose phosphate synthase (SPS) was induced by UVB stress, and SUS together with sucrose phosphatase (SPP) was increased under UVD treatment (Figure 7). SPS is the key rate-limiting enzyme of sucrose synthesis and is closely associated with starch/sucrose levels in leaves. High SPS activity represents an increase in the distribution of C in sucrose and a decrease in starch formation.[34] When plants exposed to environmental pressure, improving the abundance of SPS can promote the synthesis of sucrose, which contributes to stabilizing protein and membrane structure and function.[35] The abundance of glucan phosphorylase (GP) was increased in the UVB group (Table S1), and another starch metabolism related enzyme starch synthase (SS) was upregulated in the UVD group (Table S2). The presence of GP leads to the phosphorolytic degradation of leaf starch[36] forming glucose 1 phosphate. SS is one of the major enzymes mediating starch biosynthesis. Studies on *Oryza sativa* revealed that the decrease in SS gene expression was correlated with the decreased starch content under drought stress.[37] Under UVB single stress, *C. terniflora* may regulate osmotic homeostasis or generate energy substances to resist light stress by accumulating soluble sugars. When plants face long-term or multiple stresses, soluble sugar levels usually decrease after an initial rise. Therefore, *C. terniflora* leaves might adjust their carbohydrate balance to reduce the stress impact. The results indicated that the changes in carbohydrates and related proteins in leaves were differentially affected by UV-B and UV-D.

4.3. MAPK Signaling Pathway and Activated Hyperosmotic Response Were Triggered to Resist UV-B Radiation. Protein phosphorylation is known to alter the activity of proteins in response to environmental stimuli, signal transduction, and metabolism.[15,38] Here, phosphoproteomic analysis of *C. terniflora* leaves showed that phosphorylated proteins were involved in the MAPK signaling pathway and were significantly enriched in the UVB-treated group (Figure 4A). The MAPK pathway is a conserved signaling pathway in eukaryotes. UV-B and other abiotic factors may cause wounding on plants under environmental conditions.[39] When wounding does occur, plants respond to this damage by triggering the MAPK signaling pathway.[40] MAPKs have four clades, among which MPK3 and MPK6 belong to clade A.[40] The plant MAPK cascade influences the expression of downstream genes by passing stress signals generated during in abiotic stress.[41,42] We mapped DPPs to the MAPK signaling pathway according to the KEGG database and found that MKK4/5 and MPK3/6 cascade proteins were increased in the UVB group according to phosphoproteomic data (Figure 8, Table S3). The MKK4/5 and MPK3/6 cascades control ethylene biosynthesis to resist wounding in *Arabidopsis thaliana*.[43] Consistent with this result, another MAPK module, the type-2C protein-phosphatase (PP2C) and snf1-related protein kinase2 (SnRK2) cascade, was also affected. Abscisic acid (ABA) enables PP2C sequestration and then triggers SnRK2 activation, thereby inhibiting plant growth.[44] Nevertheless, the abundances of PP2C and SnRK2 were both reduced under UVB treatment, and the level of SnRK2 declined further, which might reduce the inhibition of growth. In addition, the hyperosmotic response could be activated by the MAPK pathway in response to a variety of stimuli. Heat stress triggers MAPK crosstalk to activate the hyperosmotic response by related protein phosphorylation.[45] Hyperosmotic response was the most significantly enriched GO term in the BP category for UVB DPPs (Figure S2A). Thus, increased hyperosmotic response proteins might contribute to the resistance of leaves against osmotic stress triggered by UV-B stress (Table S3). Additionally, abiotic stress is usually accompanied by oxidative stress. MAPK is associated with the regulation of antioxidant capacity. In tomato, the overproduction of H_2O_2 and O^{2-} was reduced after using a MAPK inhibitor under salt stress.[46] The content of T-AOC increased in the UVB stress group and decreased in the UVD stress group. Improvement of antioxidant capacity may be one of the ways to resist UV light stress. Meanwhile, combined stress might contribute to the negative effects on antioxidant capacity in *C. terniflora*.

4.4. Ca^{2+}-Related Proteins Undergo Phosphorylation/Dephosphorylation in Response to UV-B Radiation

https://doi.org/10.1021/acsomega.2c07258
ACS Omega 2023, 8, 1652−1662

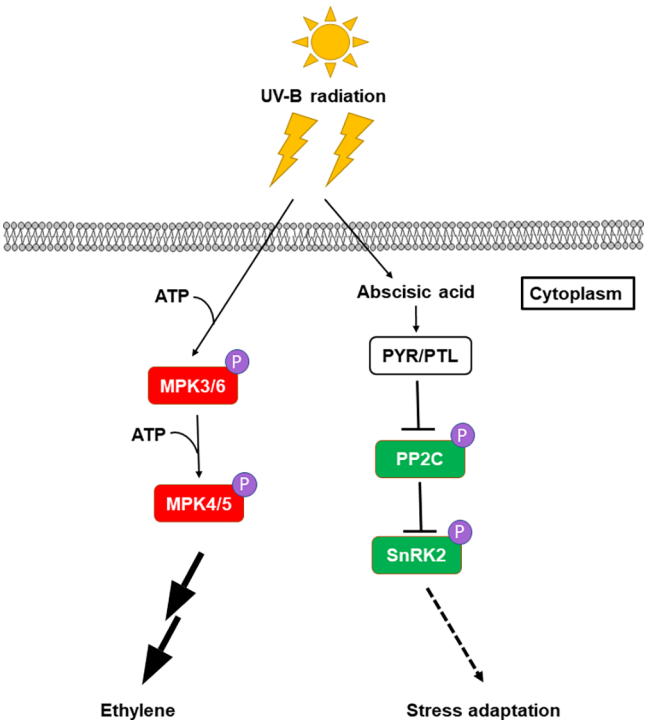

Figure 8. DPPs of UVB/CK mapped to the MAPK signaling pathway. The red blocks represent increased phosphorylated proteins, while the green blocks represent decreased phosphorylated protein.

Followed by Dark Treatment. Through the phosphorylation/dephosphorylation of kinases, the phosphorylation/dephosphorylation processes of stimuli resistance-related proteins are activated to initiate the protection response. DPPs of UVD were mainly enriched in response to stimulus, especially response to water deprivation. Water deprivation is a common reaction in various abiotic stresses. Among the proteins that respond to water deprivation, we noticed that Ca^{2+} signaling related phosphoproteins had undergone changes. Previous analysis[47] indicated that Ca^{2+} is a crucial macronutrient for plant defense responses, such as temperature shifts, light, salinity, and metalloids.[48−50] The phosphoproteomic data confirmed that Ca^{2+}-transporting ATPase was increased by UVD treatment, while Ca^{2+}-dependent protein kinase (CDPK) and calcineurin B-like protein (CBL) were decreased (Table S4). Ca^{2+}-transporting ATPase pumps Ca^{2+} ions out of the cell and binds to calmodulin in a Ca^{2+}-dependent manner.[51] CDPK and CBL are sensor proteins that reflect Ca^{2+} concentrations.[52] The CBL family is a family of plant-specific serine/threonine kinases[53] and represents a key group of Ca^{2+} transients.[54] Abiotic stress elicits a cytosolic Ca^{2+} concentration increase in a short time, and then, Ca^{2+} signatures are relayed by CBLs and CDPK.[55] CBL is involved in regulating freezing tolerance in *Solanum tuberosum*.[56] These results suggested that UV-D stress resistance in *C. terniflora* leaves might be achieved by Ca^{2+} protein phosphorylation/dephosphorylation to maintain cell Ca^{2+} homeostasis.

5. CONCLUSIONS

In this work, UV light stress damaged the photosynthetic system of *C. terniflora* leaves. Proteomics revealed that *C. terniflora* leaves adjusted carbohydrate balance in response to UVB and UVD treatment. Moreover, UVB stress activated the MAPK pathway by phosphorylating or dephosphorylating pivotal proteins and triggered a hyperosmotic response and antioxidation capability. Phosphoproteins related to Ca^{2+} signal regulation were changed significantly to resist UVD stress. In conclusion, this research provided a new reference to study the mechanism of *C. terniflora* abiotic stress resistance from phosphoproteomic combined with proteomic data.

DATA AVAILABILITY

The datasets of this study can be found in the ProteomeXchange Consortium[57] via the PRIDE[58] partner repository with identifier PXD038136 .

ASSOCIATED CONTENT

Supporting Information

The Supporting Information is available free of charge at https://pubs.acs.org/doi/10.1021/acsomega.2c07258.

Bar graph illustrating the top 20 significantly ($p < 0.05$) enriched GO terms in each category of DAPs in UVB/CK and UVD/CK; bar graph of enriched GO terms of DPPs in UVB/CK and UVD/CK; key differentially abundant proteins (DAPs) of UVB/CK; key differentially abundant proteins (DAPs) of UVD/CK; key differentially phosphorylated proteins (DPPs) of UVB/CK; and key differentially phosphorylated proteins (DPPs) of UVD/CK (PDF)

AUTHOR INFORMATION

Corresponding Authors

Bingxian Yang − *College of Life Sciences and Medicine, Zhejiang Sci-Tech University, Hangzhou 310018, China*; Email: zhuwei@ibmc.ac.cn

Wei Zhu − *The Cancer Hospital of the University of Chinese Academy of Sciences (Zhejiang Cancer Hospital), Institute of Basic Medicine and Cancer (IBMC), Chinese Academy of Sciences, Hangzhou 310022, China*; orcid.org/0000-0001-9582-3787; Email: xianyb@126.com

Authors

Minglei Tao − *College of Biomedical Engineering & Instrument Science, Zhejiang University, Hangzhou 310027, China*

Shengzhi Liu − *College of Biomedical Engineering & Instrument Science, Zhejiang University, Hangzhou 310027, China*

Amin Liu − *College of Biomedical Engineering & Instrument Science, Zhejiang University, Hangzhou 310027, China*

Yaohan Li − *College of Biomedical Engineering & Instrument Science, Zhejiang University, Hangzhou 310027, China*

Jingkui Tian − *The Cancer Hospital of the University of Chinese Academy of Sciences (Zhejiang Cancer Hospital), Institute of Basic Medicine and Cancer (IBMC), Chinese Academy of Sciences, Hangzhou 310022, China*

Complete contact information is available at: https://pubs.acs.org/10.1021/acsomega.2c07258

Author Contributions

M.T., W.Z., and B.Y. conceived the study plans. M.T., S.L., and A.L. collected samples and performed omics experiments. M.T. and Y.L. analyzed the data. M.T. performed the other mentioned experiments and wrote the paper. W.Z., J.T., and B.Y. reviewed and revised the paper. All authors read the paper and agreed to publish the manuscript.

Notes

The authors declare no competing financial interest.

https://doi.org/10.1021/acsomega.2c07258
ACS Omega 2023, 8, 1652−1662

■ ACKNOWLEDGMENTS

This work was supported by the Natural Science Foundation of Jiangsu Province (no. BK20190234).

■ REFERENCES

(1) Kawata, Y.; Kizu, H.; Tomimori, T. Studies on the constituents of Clematis species. VII. Triterpenoid saponins from the roots of Clematis terniflora DC. var. robusta Tamura. *Chem. Pharm. Bull.* **1998**, *46*, 1891−1900.

(2) Li, W. T.; Yang, B. X.; Zhu, W.; Gong, M. H.; Xu, X. D.; Lu, X. H.; Sun, L. L.; Tian, J. K.; Zhang, L. A new indole alkaloidal glucoside from the aerial parts of Clematis terniflora DC. *Nat. Prod. Res.* **2013**, *27*, 2333−2337.

(3) Tao, M.; Zhu, W.; Han, H.; Liu, S.; Liu, A.; Li, S.; Fu, H.; Tian, J. Mitochondrial proteomic analysis reveals the regulation of energy metabolism and reactive oxygen species production in Clematis terniflora DC. leaves under high-level UV-B radiation followed by dark treatment. *J. Proteomics* **2022**, *254*, 104410.

(4) Chen, R. Z.; Cui, L.; Guo, Y. J.; Rong, Y. M.; Lu, X. H.; Sun, M. Y.; Zhang, L.; Tian, J. K. In vivo study of four preparative extracts of Clematis terniflora DC. for antinociceptive activity and anti-inflammatory activity in rat model of carrageenan-induced chronic non-bacterial prostatitis. *J. Ethnopharmacol.* **2011**, *134*, 1018−1023.

(5) Yi, Y.; Zhang, L.-h.; Yang, B.-x.; Tian, J.-k.; Lin, Z. Aurantiamide acetate suppresses the growth of malignant gliomas in vitro and in vivo by inhibiting autophagic flux. *J. Cell. Mol. Med.* **2015**, *19*, 1055−1064.

(6) Ma, M.; Wang, P.; Yang, R.; Zhou, T.; Gu, Z. UV-B mediates isoflavone accumulation and oxidative-antioxidant system responses in germinating soybean. *Food Chem.* **2019**, *275*, 628−636.

(7) Zhong, Z.; Liu, S.; Zhu, W.; Ou, Y.; Yamaguchi, H.; Hitachi, K.; Tsuchida, K.; Tian, J.; Komatsu, S. Phosphoproteomics Reveals the Biosynthesis of Secondary Metabolites in Catharanthus roseus under Ultraviolet-B Radiation. *J. Proteome Res.* **2019**, *18*, 3328−3341.

(8) Takshak, S.; Agrawal, S. B. Defence strategies adopted by the medicinal plant Coleus forskohlii against supplemental ultraviolet-B radiation: Augmentation of secondary metabolites and antioxidants. *Plant Physiol. Biochem.* **2015**, *97*, 124−138.

(9) Liu, A.; Liu, S.; Li, Y.; Tao, M.; Han, H.; Zhong, Z.; Zhu, W.; Tian, J. Phosphoproteomics Reveals Regulation of Secondary Metabolites in Mahonia bealei Exposed to Ultraviolet-B Radiation. *Front. Plant Sci.* **2021**, *12*, 794906.

(10) Csepregi, K.; Coffey, A.; Cunningham, N.; Prinsen, E.; Hideg, É.; Jansen, M. A. K. Developmental age and UV-B exposure co-determine antioxidant capacity and flavonol accumulation in Arabidopsis leaves. *Environ. Exp. Bot.* **2017**, *140*, 19−25.

(11) Yang, B.; Wang, X.; Gao, C.; Chen, M.; Guan, Q.; Tian, J.; Komatsu, S. Proteomic and Metabolomic Analyses of Leaf from Clematis terniflora DC. Exposed to High-Level Ultraviolet-B Irradiation with Dark Treatment. *J. Proteome Res.* **2016**, *15*, 2643−2657.

(12) Wu, L.; Meng, X.; Huang, H.; Liu, Y.; Jiang, W.; Su, X.; Wang, Z.; Meng, F.; Wang, L.; Peng, D.; Xing, S. Comparative Proteome and Phosphoproteome Analyses Reveal Different Molecular Mechanism Between Stone Planting Under the Forest and Greenhouse Planting of Dendrobium huoshanense. *Front. Plant Sci.* **2022**, *13*, 937392.

(13) Yin, C.; Sun, Z.; Ji, C.; Li, F.; Wu, H. Toxicological effects of tris(1,3-dichloro-2-propyl) phosphate in oyster Crassostrea gigas using proteomic and phosphoproteomic analyses. *J. Hazard. Mater.* **2022**, *434*, 128824.

(14) Sabila, M.; Kundu, N.; Smalls, D.; Ullah, H. Tyrosine Phosphorylation Based Homo-dimerization of Arabidopsis RACK1A Proteins Regulates Oxidative Stress Signaling Pathways in Yeast. *Front. Plant Sci.* **2016**, *7*, 176.

(15) Balotf, S.; Wilson, C. R.; Tegg, R. S.; Nichols, D. S.; Wilson, R. Large-Scale Protein and Phosphoprotein Profiling to Explore Potato Resistance Mechanisms to Spongospora subterranea Infection. *Front. Plant Sci.* **2022**, *13*, 872901.

(16) Xing, J.; Tan, J.; Feng, H.; Zhou, Z.; Deng, M.; Luo, H.; Deng, Z. Integrative Proteome and Phosphoproteome Profiling of Early Cold Response in Maize Seedlings. *Int. J. Mol. Sci.* **2022**, *23*, 6493.

(17) Zhu, W.; Han, H.; Liu, A.; Guan, Q.; Kang, J.; David, L.; Dufresne, C.; Chen, S.; Tian, J. Combined ultraviolet and darkness regulation of medicinal metabolites in Mahonia bealei revealed by proteomics and metabolomics. *J. Proteomics* **2021**, *233*, 104081.

(18) Zhong, Z.; Liu, S.; Han, S.; Li, Y.; Tao, M.; Liu, A.; He, Q.; Chen, S.; Dufresne, C.; Zhu, W.; Tian, J. Integrative omic analysis reveals the improvement of alkaloid accumulation by ultraviolet-B radiation and its upstream regulation in Catharanthus roseus. *Ind. Crops Prod.* **2021**, *166*, 113448.

(19) Yang, B.; Guan, Q.; Tian, J.; Komatsu, S. Data for transcriptomic and proteomic analyses of leaves from Clematis terniflora DC. under binary stress. *Data Brief* **2017**, *12*, 138−142.

(20) Cantalapiedra, C. P.; Hernández-Plaza, A.; Letunic, I.; Bork, P.; Huerta-Cepas, J. eggNOG-mapper v2: Functional Annotation, Orthology Assignments, and Domain Prediction at the Metagenomic Scale. *Mol. Biol. Evol.* **2021**, *38*, 5825−5829.

(21) Chen, C.; Chen, H.; Zhang, Y.; Thomas, H. R.; Frank, M. H.; He, Y.; Xia, R. TBtools: An Integrative Toolkit Developed for Interactive Analyses of Big Biological Data. *Mol. Plant* **2020**, *13*, 1194−1202.

(22) Bu, D.; Luo, H.; Huo, P.; Wang, Z.; Zhang, S.; He, Z.; Wu, Y.; Zhao, L.; Liu, J.; Guo, J.; Fang, S.; Cao, W.; Yi, L.; Zhao, Y.; Kong, L. KOBAS-i: intelligent prioritization and exploratory visualization of biological functions for gene enrichment analysis. *Nucleic Acids Res.* **2021**, *49*, W317−W325.

(23) Yan, Q.; Zhao, L.; Wang, W.; Pi, X.; Han, G.; Wang, J.; Cheng, L.; He, Y.-K.; Kuang, T.; Qin, X.; Sui, S.-F.; Shen, J.-R. Antenna arrangement and energy-transfer pathways of PSI−LHCI from the moss Physcomitrella patens. *Cell Discovery* **2021**, *7*, 10.

(24) Zhang, Y.; Li, B.; Liu, F.; Luo, P.; Wang, Y.; Liu, D.; Wu, X.; Zhang, Z.; Wu, J. Transcriptomic and physiological analysis revealed the ammonium tolerance mechanisms of Myriophyllum aquaticum. *Environ. Exp. Bot.* **2021**, *187*, 104462.

(25) Meng, X.; Zhang, Y.; Wang, N.; He, H.; Wen, B.; Zhang, R.; Fu, X.; Xiao, W.; Li, D.; Li, L.; Chen, X. Genome-wide identification and characterization of the Prunus persica ferredoxin gene family and its role in improving heat tolerance. *Plant Physiol. Biochem.* **2022**, *179*, 108−119.

(26) Kimata-Ariga, Y.; Nishimizu, Y.; Shinkoda, R. Molecular mechanism of negative cooperativity of ferredoxin-NADP + reductase by ferredoxin and NADP(H): role of the ion pair of ferredoxin Arg40 of and FNR Glu154. *J. Biochem.* **2022**, *172*, 377.

(27) Li, C.; Hu, Y.; Huang, R.; Ma, X.; Wang, Y.; Liao, T.; Zhong, P.; Xiao, F.; Sun, C.; Xu, Z.; Deng, X.; Wang, P. Mutation of FdC2 gene encoding a ferredoxin-like protein with C-terminal extension causes yellow-green leaf phenotype in rice. *Plant Sci.* **2015**, *238*, 127−134.

(28) Stuart, D.; Sandström, M.; Youssef, H. M.; Zakhrabekova, S.; Jensen, P. E.; Bollivar, D.; Hansson, M. Barley Viridis-k links an evolutionarily conserved C-type ferredoxin to chlorophyll biosynthesis. *Plant Cell* **2021**, *33*, 2834−2849.

(29) Rodriguez-Heredia, M.; Saccon, F.; Wilson, S.; Finazzi, G.; Ruban, A. V.; Hanke, G. T. Protection of photosystem I during sudden light stress depends on ferredoxin:NADP(H) reductase abundance and interactions. *Plant Physiol.* **2021**, *188*, 1028−1042.

(30) Rodriguez, R. E.; Lodeyro, A.; Poli, H. O.; Zurbriggen, M.; Peisker, M.; Palatnik, J. F.; Tognetti, V. B.; Tschiersch, H.; Hajirezaei, M.-R.; Valle, E. M.; Carrillo, N. Transgenic Tobacco Plants Overexpressing Chloroplastic Ferredoxin-NADP(H) Reductase Display Normal Rates of Photosynthesis and Increased Tolerance to Oxidative Stress. *Plant Physiol.* **2007**, *143*, 639−649.

(31) Sami, F.; Yusuf, M.; Faizan, M.; Faraz, A.; Hayat, S. Role of sugars under abiotic stress. *Plant Physiol. Biochem.* **2016**, *109*, 54−61.

(32) Rosa, M.; Prado, C.; Podazza, G.; Interdonato, R.; González, J. A.; Hilal, M.; Prado, F. E. Soluble sugars. *Plant Signaling Behav.* **2009**, *4*, 388−393.

(33) Cho, Y. H.; Yoo, S. D.; Sheen, J. Regulatory functions of nuclear hexokinase1 complex in glucose signaling. *Cell* **2006**, *127*, 579−589.

https://doi.org/10.1021/acsomega.2c07258
ACS Omega 2023, 8, 1652−1662

(34) Huber, S. C.; Rufty, T. W.; Kerr, P. S., Effect of Photoperiod on Photosynthate Partitioning and Diurnal Rhythms in Sucrose Phosphate Synthase Activity in Leaves of Soybean (Glycine max L. [Merr.]) and Tobacco (Nicotiana tabacum L.) 1. Plant Physiology 1984, *75* (4), 1080−1084, DOI: 10.1104/pp.75.4.1080.
(35) Lunn, J. E. Evolution of Sucrose Synthesis. *Plant Physiol.* **2002**, *128*, 1490−1500.
(36) Ceusters, N.; Ceusters, J.; Hurtado-Castano, N.; Dever, L. V.; Boxall, S. F.; Kneřová, J.; Waller, J. L.; Rodick, R.; Van den Ende, W.; Hartwell, J.; Borland, A. M. Phosphorolytic degradation of leaf starch via plastidic α-glucan phosphorylase leads to optimized plant growth and water use efficiency over the diel phases of Crassulacean acid metabolism. *J. Exp. Bot.* **2021**, *72*, 4419−4434.
(37) Vee, P.; Tyagi, A. Correlation between expression and activity of ADP glucose pyrophosphorylase and starch synthase and their role in starch accumulation during grain filling under drought stress in rice. *Plant Physiol. Biochem.* **2020**, *157*, 239−243.
(38) Guo, J.; Li, S.; Brestic, M.; Li, N.; Zhang, P.; Liu, L.; Li, X. Modulations in protein phosphorylation explain the physiological responses of barley (Hordeum vulgare) to nanoplastics and ZnO nanoparticles. *J. Hazard. Mater.* **2023**, *443*, 130196.
(39) Colcombet, J.; Hirt, H. Arabidopsis MAPKs: a complex signalling network involved in multiple biological processes. *Biochem. J.* **2008**, *413*, 217−226.
(40) Sözen, C.; Schenk, S. T.; Boudsocq, M.; Chardin, C.; Almeida-Trapp, M.; Krapp, A.; Hirt, H.; Mithöfer, A.; Colcombet, J. Wounding and Insect Feeding Trigger Two Independent MAPK Pathways with Distinct Regulation and Kinetics. *Plant Cell* **2020**, *32*, 1988−2003.
(41) Zhao, C.; Wang, P.; Si, T.; Hsu, C. C.; Wang, L.; Zayed, O.; Yu, Z.; Zhu, Y.; Dong, J.; Tao, W. A.; Zhu, J. K. MAP Kinase Cascades Regulate the Cold Response by Modulating ICE1 Protein Stability. *Dev. Cell* **2017**, *43*, 618−629.e5.
(42) Takahashi, Y.; Zhang, J.; Hsu, P. K.; Ceciliato, P. H. O.; Zhang, L.; Dubeaux, G.; Munemasa, S.; Ge, C.; Zhao, Y.; Hauser, F.; Schroeder, J. I. MAP3Kinase-dependent SnRK2-kinase activation is required for abscisic acid signal transduction and rapid osmotic stress response. *Nat. Commun.* **2020**, *11*, 12.
(43) Li, S.; Han, X.; Yang, L.; Deng, X.; Wu, H.; Zhang, M.; Liu, Y.; Zhang, S.; Xu, J. Mitogen-activated protein kinases and calcium-dependent protein kinases are involved in wounding-induced ethylene biosynthesis in Arabidopsis thaliana. *Plant, Cell Environ.* **2018**, *41*, 134−147.
(44) Belda-Palazón, B.; Adamo, M.; Valerio, C.; Ferreira, L. J.; Confraria, A.; Reis-Barata, D.; Rodrigues, A.; Meyer, C.; Rodriguez, P. L.; Baena-González, E. A dual function of SnRK2 kinases in the regulation of SnRK1 and plant growth. *Nature Plants* **2020**, *6*, 1345−1353.
(45) Dunayevich, P.; Baltanás, R.; Clemente, J. A.; Couto, A.; Sapochnik, D.; Vasen, G.; Colman-Lerner, A. Heat-stress triggers MAPK crosstalk to turn on the hyperosmotic response pathway. *Sci. Rep.* **2018**, *8*, 15168.
(46) Wei, L.; Feng, L.; Liu, Y.; Liao, W. Mitogen-Activated Protein Kinase Is Involved in Salt Stress Response in Tomato (Solanum lycopersicum) Seedlings. *Int. J. Mol. Sci.* **2022**, *23*, 7645.
(47) Tong, T.; Li, Q.; Jiang, W.; Chen, G.; Xue, D.; Deng, F.; Zeng, F.; Chen, Z.-H. Molecular Evolution of Calcium Signaling and Transport in Plant Adaptation to Abiotic Stress. *Int. J. Mol. Sci.* **2021**, 12308.
(48) Xiong, L.; Schumaker, K. S.; Zhu, J. K. Cell signaling during cold, drought, and salt stress. *Plant Cell* **2002**, *14*, S165−S183.
(49) Chen, X.; Jiang, W.; Tong, T.; Chen, G.; Zeng, F.; Jang, S.; Gao, W.; Li, Z.; Mak, M.; Deng, F.; Chen, Z.-H. Molecular Interaction and Evolution of Jasmonate Signaling With Transport and Detoxification of Heavy Metals and Metalloids in Plants. *Front. Plant Sci.* **2021**, 665842.
(50) Lee, H. J.; Seo, P. J. Ca^{2+}talyzing Initial Responses to Environmental Stresses. *Trends Plant Sci.* **2021**, *26*, 849−870.
(51) Strehler, E. E., Plasma Membrane Calcium-Transporting ATPase. In *Encyclopedia of Signaling Molecules*; Choi, S., Ed. Springer New York: New York, NY, 2016; pp. 1−8.
(52) Atif, R. M.; Shahid, L.; Waqas, M.; Ali, B.; Rashid, M. A. R.; Azeem, F.; Nawaz, M. A.; Wani, S. H.; Chung, G. Insights on Calcium-Dependent Protein Kinases (CPKs) Signaling for Abiotic Stress Tolerance in Plants. *Int. J. Mol. Sci.* **2019**, *20*, 5298.
(53) Poddar, N.; Deepika, D.; Chitkara, P.; Singh, A.; Kumar, S. Molecular and expression analysis indicate the role of CBL interacting protein kinases (CIPKs) in abiotic stress signaling and development in chickpea. *Sci. Rep.* **2022**, *12*, 16862.
(54) Batistic, O.; Kudla, J. Plant calcineurin B-like proteins and their interacting protein kinases. *Biochim. Biophys. Acta* **2009**, *1793*, 985−992.
(55) Gong, Z.; Xiong, L.; Shi, H.; Yang, S.; Herrera-Estrella, L. R.; Xu, G.; Chao, D. Y.; Li, J.; Wang, P. Y.; Qin, F.; Li, J.; Ding, Y.; Shi, Y.; Wang, Y.; Yang, Y.; Guo, Y.; Zhu, J. K. Plant abiotic stress response and nutrient use efficiency. *Sci. China: Life Sci.* **2020**, *63*, 635−674.
(56) Chen, L.; Zhao, H.; Chen, Y.; Jiang, F.; Zhou, F.; Liu, Q.; Fan, Y.; Liu, T.; Tu, W.; Walther, D.; Song, B. Comparative transcriptomics analysis reveals a calcineurin B-like gene to positively regulate constitutive and acclimated freezing tolerance in potato. *Plant, Cell Environ.* **2022**, *45*, 3305−3321.
(57) Deutsch, E. W.; Nuno, B.; Vagisha, S.; Yasset, P. R.; Carver, J. J.; Kundu, D. J.; David, G. S.; Jarnuczak, A. F.; Suresh, H.; Pullman, B. The ProteomeXchange consortium in 2020: enabling 'big data' approaches in proteomics. *Nucleic Acids Res.* **2019**, *48*, D1145−D1152.
(58) Yasset, P. R.; Attila, C.; Bai, J.; Manuel, B. L.; Suresh, H.; Kundu, D. J.; Avinash, I.; Johannes, G.; Gerhard, M.; Martin, E. The PRIDE database and related tools and resources in 2019: improving support for quantification data. *Nucleic Acids Res.* **2018**, *D1*, D1.

https://doi.org/10.1021/acsomega.2c07258
ACS Omega 2023, 8, 1652−1662